Hamiltonian monodromy, its manifestations and generalizations

Boris Zhilinskii
Université du Littoral Côte d'Opale, MREI 2,
189A, av. M. Schumann, Dunkerque, 59140 France
email : zhilin@univ-littoral.fr

April 3, 2010

Abstract

Hamiltonian monodromy is known to be the simplest obstruction to the existence of global action-angle variables in integrable models of classical dynamics. Recently, the corresponding quantum monodromy concept is introduced and shown to be an important qualitative feature of many different realistic models and concrete physical quantum systems. Vibrational structure of simple molecules, electronic states of hydrogen atom in external fields, coupling of angular momenta is discussed as basic physical examples. Starting from these examples new qualitative features of molecular systems leading naturally to generalized monodromy notions is introduced. Going finally to really complex systems the tentative relation between phyllotaxis and monodromy is suggested.

1 Introduction

The idea of the present paper is to demonstrate new qualitative features which were found recently in different relatively simple quantum atomic and molecular systems, namely, I speak about quantum Hamiltonian monodromy and its generalizations. In classical mechanics, the Hamiltonian monodromy was initially considered in the context of completely integrable Hamiltonian systems as the first obstruction to the existence of global action variables [52, 18]. Its differential geometry meaning was not appreciated by physicists at the beginning and the Hamiltonian monodromy was treated as mathematical curiosity which apparently does not lead to interesting physical or any other natural science applications. Only after more than 15 years of intensive popularization of the monodromy notion by Richard Cushman at interdisciplinary physics-chemistry-mathematics conferences and in his book [8], the monodromy subject became rather popular, especially in molecular science. This success of monodromy was mainly due to the formulation of the quantum version of Hamiltonian monodromy [9, 69, 59] and the discovery of quantum Hamiltonian monodromy in many different real physical systems [11, 23, 7, 30, 72]. Recent proof of the persistence of monodromy under small perturbations spoiling the integrability [6] strengthens the interest of applications to real (typically non-integrable) systems.

The simplest way to see Hamiltonian monodromy is to construct the so called momentum or energy-momentum map for an completely integrable (for simplicity two-dimensional) Hamiltonian system [2, 8, 36, 5]. This is a map from the classical phase space to the space of values of integrals of motion (see figure 1). It allows us to consider the classical phase space as (generically singular) fibration with the base space being the space of values of integrals of motion and fibers being the inverse images of the map. The image of the map consists of regular and singular values. The inverse images of regular values are regular tori [2], while singular values correspond to topologically different singular tori. Several examples of singular fibers are represented in figure 2.

In the simplest case the Hamiltonian monodromy is due to the generic presence of a singular fiber, so called pinched torus (figure 2, a), which manifests itself in the image of the energy-momentum map as an isolated singular value (see figure 1, a). This situation is often referenced as focus-focus singularity [49, 43].

In higher dimensional problems the singular fiber of the pinched torus type is a generic singularity of codimension 2. This means that for completely integrable $3D$-degree of freedom Hamiltonian systems

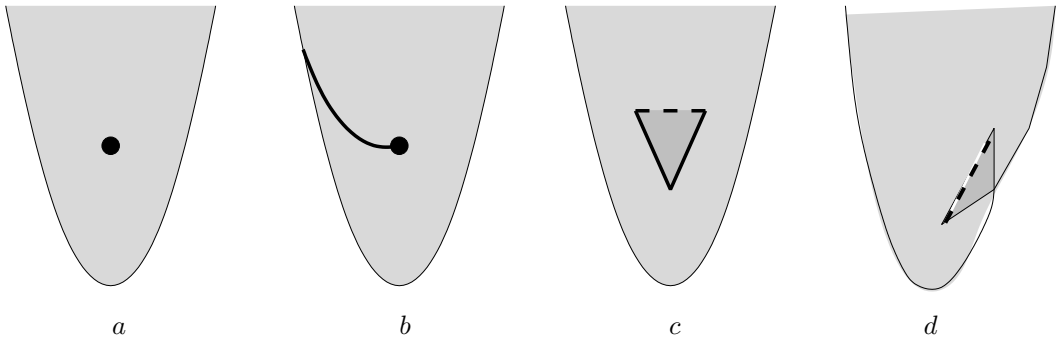

Figure 1: Typical images of the energy momentum map for completely integrable Hamiltonian systems with two degree of freedom in the case of: (a) - integer monodromy; (b) - fractional monodromy; (c) - nonlocal monodromy; (d) - bidromy. Values in light shaded area lift to single regular 2-tori; values in dark shaded area lift to two regular 2-tori. Black point in subfigure a corresponds to pinched torus shown in figure 2 (a). Each point of thick solid line in subfigure (b) corresponds to curled torus (see figure 2 b). Each point of dash line in subfigures (c) and (d) corresponds to bitorus shown in figure 2 c. Each of two cuspidal points in subfigures (c) and (d) associated with the end of bitorus line correspond to singular torus represented in figure 2 d.

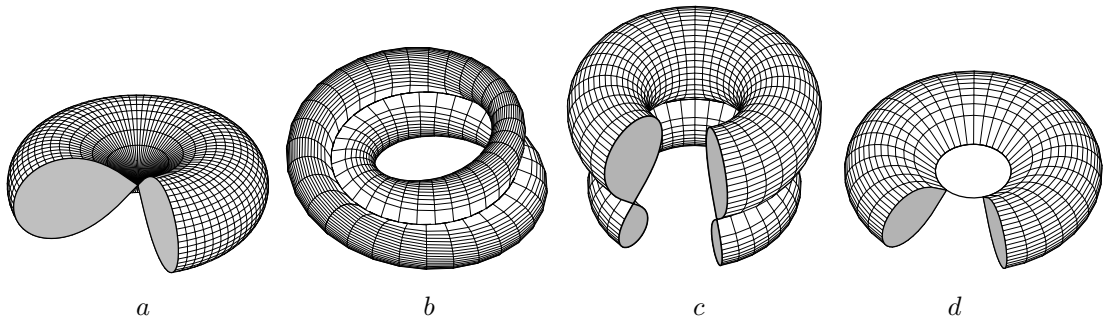

Figure 2: Two dimensional singular fibers in the case of integrable Hamiltonian systems with two degrees of freedom: a - pinched torus, b - curled torus, c - bitorus, and d - singular torus.

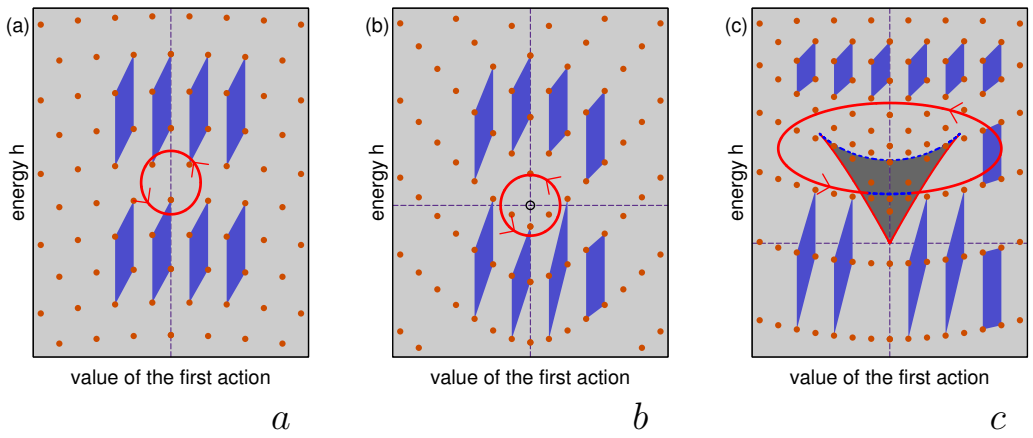

Figure 3: Quantum joint spectra for typical regions of the image of energy - momentum map for integrable problems. *a* - a region of regular values. *b* - region around a singular value of the classical map, associated with pinched torus. *c* - neighborhood of a two-component region of the classical map (dark curvilinear triangle).

we typically meet lines of singular values whose points correspond to singular (pinched) tori (or to focus-focus singularities). The appearance of codimension 3 and higher singularities in physically relevant dynamical systems remains till now an open question [3, 33, 34, 35]

The completely integrable toric fibration allows existence of local action variables in any simply connected region of regular values of the energy-momentum map. At the same time global action variables do not exist in a non-simply connected region of regular values surrounding the critical value(s) of the energy-momentum map associated, in particular, with the pinched torus. The monodromy of the classical integrable Hamiltonian system is defined as an automorphism of the first homology group of a regular fiber after continuation of basic cycles along a closed contour going through regular values and surrounding singular value of the momentum map in the base space of the integrable fibration.

Very simple and clear manifestation of the Hamiltonian monodromy can be seen on pictures showing simultaneously the image of the classical energy momentum map and the corresponding joint spectrum of mutually commuting quantum observables, i.e. the lattice formed by common eigenvalues of mutually commuting operators [59]. Simple Bohr quantization rules together with existence of local action variables lead to appearance of a local regular lattice of common eigenvalues of mutually commuting operators in any simply connected region of the image of classical energy-momentum map, corresponding to regular values of the map (see figure 3, *a*). At the same time, going with elementary cell of so obtained lattice of common quantum eigenvalues along a non-contractible closed path surrounding critical value results in a modification of the elementary cell.

Figure 3 demonstrates evolution of an elementary cell after going along a closed path surrounding either isolated singularity (3, *b*) or the whole two-component region (3, *c*) on the $2D$-image of the energy-momentum map. The matrix relating initial and final cell is a quantum monodromy 2×2 matrix with integer entries. It is inverse conjugated (dual) to classical monodromy matrix giving the transformation of the basis cycles of the first homology group. It is clear, that the basis of the regular lattice in the quantum case, or of the homology group in the classical case, can be chosen in an ambiguous way, up to similarity transformation with an arbitrary matrix from $SL(2, Z)$, the special group of 2×2 matrices with integer entries. Due to this ambiguity the monodromy matrix is defined as a class of conjugated elements of $SL(2, Z)$ or $GL(2, Z)$ and the particular "normal form" can be chosen to represent each class of conjugated elements.

One of fundamental physical problems which clearly shows the presence of monodromy is the hydrogen atom under the presence of weak external electric and magnetic fields [11]. Figure 4 shows the joint spectrum and the image of the corresponding classical energy-momentum map for the integrable approximation for this problem for some specific values of external orthogonal fields. The analysis of the joint quantum lattice clearly indicates the presence of doubly pinched torus as a singular fiber.

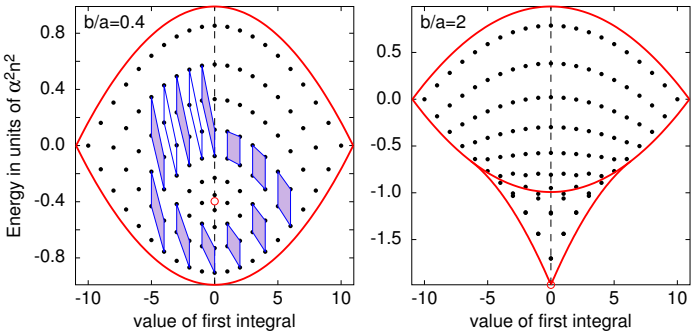

Figure 4: Joint spectrum of two commuting quantum operators for effective Hamiltonian describing splitting of an n-shell of the hydrogen atom in the presence of two orthogonal static electric and magnetic fields [11]. The parameters of external fields are chosen to demonstrate: (Left) - the presence of an isolated singular fiber (doubly pinched torus); (Right) - the presence of two-component region on the energy momentum map. Points in lower triangular region are, in fact, doubly degenerate. Their splitting is seen in the near separatrix region.

2 Monodromy and redistribution of energy levels

In order to see an interesting relation between monodromy and the phenomenon of the redistribution of energy levels between different energy bands the following simple model problem is extremely useful. To write it explicitly let us introduce two kind of dynamic variables: orbital angular momentum $\mathbf{N} = (N_x, N_y, N_z)$ and spin $\mathbf{S} = (S_x, S_y, S_z)$. We assume now that N^2 and S^2 are fixed (are integrals of motion) and we take into account two competitive interactions: spin-orbit coupling $\gamma\mathbf{NS}$ and spin-external magnetic field interaction $(1-\gamma)S_z$. The resulting Hamiltonian depends on one control parameter γ:

$$H = (1-\gamma)S_z \ + \ \gamma(\mathbf{N}\cdot\mathbf{S}). \tag{1}$$

From the classical mechanics point of view this problem has two degrees of freedom with classical phase space being the product of two two-dimensional spheres $S^2 \times S^2$. Each sphere S^2 is defined in the respective 3-space (S_x, S_y, S_z) and (N_x, N_y, N_z) as $S_x^2 + S_y^2 + S_z^2 = |\mathbf{S}|^2$, $N_x^2 + N_y^2 + N_z^2 = |\mathbf{N}|^2$. Both $\mathbf{N}$ and $\mathbf{S}$ generate each a standard $so(3)$ algebra, so that

$$\{N_\alpha, N_\beta\} = \varepsilon_{\alpha\beta\gamma}N_\gamma; \quad \{S_\alpha, S_\beta\} = \varepsilon_{\alpha\beta\gamma}S_\gamma; \quad \{N_\alpha, S_\beta\} = 0.$$

One integral of motion, $J_z = N_z + S_z$ is due to the presence of axial symmetry of the problem. Together with energy, this gives completely integrable problem with compact phase space. The axial symmetry can be removed by means of singular reduction [8]. The singular reduction is necessary because the action of the $SO(2)$ symmetry group on $S^2 \times S^2$ classical phase space has four fixed points [59]. The reduction leads to a family of reduced phase spaces P_J parametrized by the value of J_z. Several members in this family P_J are singular spaces and exactly these singular spaces are of primary interest for the study of Hamiltonian monodromy [59].

From the quantum mechanics point of view we can interpret the same problem in the case of quantum number of spin $S = 1/2$ as a two state problem with the internal structure of each state being associated with N_α dynamic variables and giving consequently two energy bands. To reach physically reasonable description it is sufficient to suppose that the splitting of energy levels within each band is small compared to energy separation between bands. In an equivalent way we can speak about "slow" subsystem and "fast" subsystem. It is natural to associate the slow subsystem with the N_α dynamic variables and the fast subsystem with the S_α dynamic variables. The slow motion is responsible for the internal structure of bands. The big N value leads to a large number of quantum states within the band. The fast motion is responsible for formation of bands themselves. Taking $S = 1/2$ results in existence of only two bands.

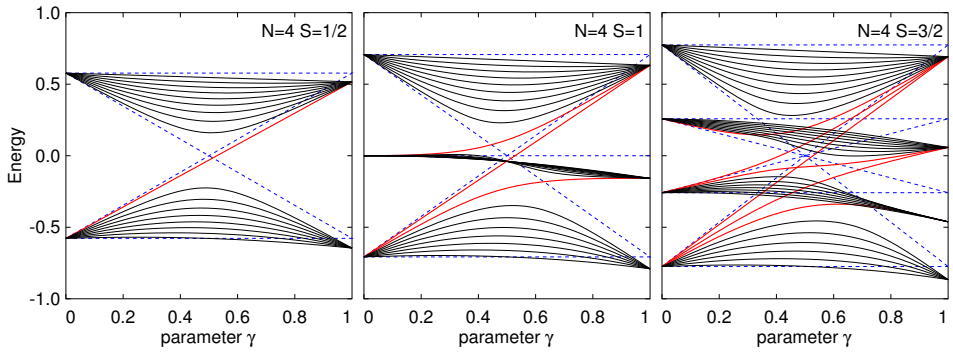

Figure 5: Redistribution of energy levels between energy bands under variation of one control parameter for model Hamiltonian (1) for $S = 1/2$, $S = 1$, and $S = 3/2$ cases and $N = 4$.

Two natural limits, namely $\gamma = 0$ and $\gamma = 1$, correspond to extremely simple Hamiltonians, possessing each two degenerate energy levels. Each degenerate energy level represents collapsed energy band. At the same time, an important feature is the difference between the number of quantum levels in bands when one compare the $\gamma = 0$ and the $\gamma = 1$ limits. Two bands at $\gamma = 0$ include each $(2N + 1)$ quantum levels, while at $\gamma = 1$ one bands includes $(2N + 2)$ and another $(2N)$ energy levels. The immediate conclusion is: the variation of the control parameter γ from 0 to 1 results in the redistribution of energy levels between bands. The presence of axial symmetry allows one to find exact solution of quantum problem in the case of $S = 1/2$ and arbitrary N and γ because the symmetry enables one to split the complete problem into several two-dimensional matrix problems corresponding to different irreducible representations of axial symmetry group. Figure 5 shows the phenomenon of the redistribution of energy levels between bands under the variation of one control parameter.

The transformation between uncoupled and coupled angular momenta explains easily the distribution of energy levels between bands in two limiting cases. Nevertheless, the problem (1) has much more general meaning. Initially this problem was suggested to relate the redistribution phenomenon with the formation of so called diabolic points in the semi-quantum model [56]. The semi-quantum model means that "fast" variables are treated as quantum ones, while "slow" variables are considered as purely classical. In semi-quantum approach, the initial complete quantum Hamiltonian becomes matrix Hamiltonian with its matrix elements being functions of classical variables and the dimension of the matrix being defined by the number of quantum states taken into account. The redistribution phenomenon was conjecturally related in [56] with the modification of the topological invariant, Chern number. But it is only after more than ten years that this conjecture was mathematically justified [26, 27] and the mathematical model relating the redistribution phenomenon and the modification of Chern classes of corresponding vector bundles constructed within the semi-quantum model was formulated and even generalized to problems with higher dimensional space of slow variables [28]. The general idea is to describe the quantum K-state system together with the classical compact reduced phase space responsible for the internal structure of isolated bands as a complex vector bundle of rang K. The base of this vector bundle is the classical reduced phase space for "slow" classical variables. Over each point of this base the complex fiber is the space of quantum eigenfunctions associated with given classical manifold. It turns out that Chern classes of vector bundles have very clear physical interpretation in terms of the number-of-state function of the band [26, 27]. This relation was demonstrated in details for vector bundles over $CP_1 \sim S^2$ but the corresponding analysis for higher-dimensional base spaces is not yet fully explored.

In order to see the relation of the redistribution phenomenon with the monodromy, we need to treat the same problem (1) within purely classical approach [59, 32]. As soon as the problem is completely integrable we can easily construct the image of the energy momentum map and analyze its evolution along with the variation of the control parameter γ between two limits corresponding to different distribution of energy levels between bands.

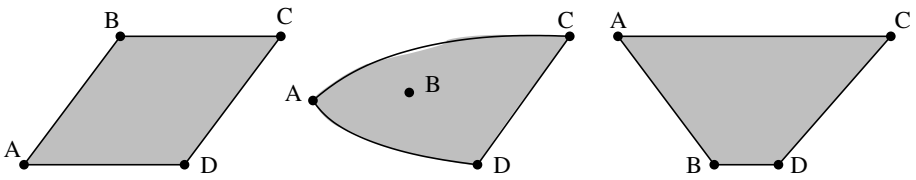

Figure 6: Qualitative modification of the image of EM map due to Hamiltonian Hopf bifurcations. Left and right: two simplest integrable toric fibrations over $S^2 \times S^2$ classical phase space corresponding to uncoupled and coupled angular momenta; A, B, C, D - critical values corresponding to singular S^0 fibers; regular points on the boundary correspond to S^1 fibers; regular internal points are regular T^2 fibers. Middle: Appearance of an isolated critical value inside the field of regular values. Critical value B corresponds to pinched torus.

Two limiting cases correspond to images of energy momentum map which differ among themselves by the location of singular values on the boundary of the image (see figure 6, left and right). The continuous transformation between these two limiting cases under variation of the control parameter γ forces one of the singular values (namely point B in figure 6) to go from the upper boundary to the lower boundary. On its way from one boundary to another the singular value becomes an isolated critical value (figure 6, middle) which corresponds to pinched torus. Appearance and disappearance of the pinched torus occurs when the point B leaves (or returns to) the boundary. This qualitative transformation of the image of the energy-momentum map is due to Hamiltonian Hopf bifurcation [71, 21]. From the other side, the modification of band structure (redistribution phenomenon) requires the qualitative transformation of the energy-momentum image (which is called also a bifurcation diagram) and this should be done by going through the region of the parameter γ values associated with the presence of an isolated critical value, and consequently with the presence of Hamiltonian monodromy. As it is shown in [59], the interval $\Delta\gamma$ of values of control parameters corresponding to the presence of an isolated critical value becomes very narrow ($\Delta\gamma \ll 1$) in the case of $S \ll N$, i.e. in the semi-quantum limit.

3 Monodromy as defect of lattices

The visualization of monodromy on the joint quantum spectrum of two commuting quantum observables by looking at the evolution of an elementary cell going around singularities of corresponding classical bifurcation diagram [59] provokes immediately a question about possible relation between singularities of integrable Hamiltonian fibrations and defects of regular lattices [74, 73, 55]. Description of different defects of periodic structures is a rather popular subject in solid state and soft matter physics [50, 41, 42]. Unfortunately, the most typical solid state defects, like dislocations or disclination, do not result in the same organization of lattice around a defect as an organization of joint quantum spectrum around generic singularity associated with classical (pinched torus) singular fiber. Nevertheless, we can follow the general idea of the defect description which is based on the "cut and glue" construction of the defect starting from the regular lattice in order to find the geometric representation of singularities of classical toric fibrations on quantum state lattices.

The representation of the "elementary monodromy" defect consists of removing from the regular lattice a specially chosen solid wedge and identifying points on two boundaries of the so obtained cut. This construction is shown in figure 7 represented in a local action variables. The crucial points of this construction are: values of local action variables at two boundaries of the cut are different, but the directions of "constant action" lines remains the same; the number of removed points from each reduced subspace with fixed action value is a linear (piece-wise) function of the value of this integral. The last property reflects the Duistermaat-Heckman statement [19, 36] about the piece-wise polynomial behavior of the volume of the reduced phase space.

Another possibility of the representation of the "elementary monodromy" defect is based on making a cut along the so called "eigenray" [66]. The eigenray is uniquely defined and after making the cut the values of local actions on two boundaries remain the same but the direction of "constant local

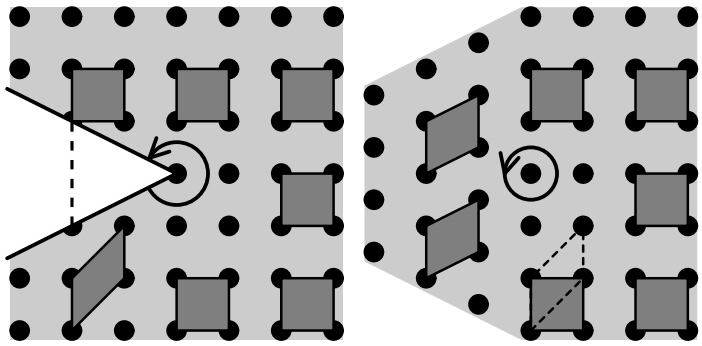

Figure 7: Construction of the "elementary monodromy" defect starting from the regular Z^2 lattice. Respective points lying on two boundaries of the removed wedge (left subfigure) are to be identified. This gives the lattice with defect (right subfigure). Dark grey quadrangles show the evolution of an elementary lattice cell along a closed path surrounding the defect point.

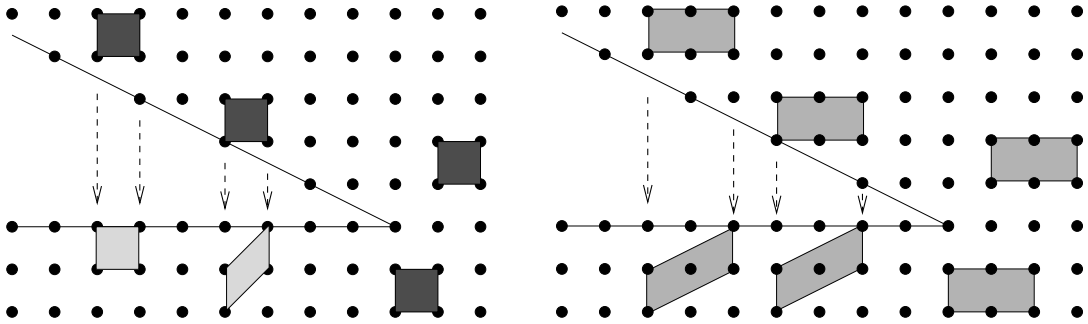

Figure 8: Construction of $1:2$ rational lattice defect. Left: Elementary cell does not pass. Right: Double cell passes. unambiguously.

action" lines should be changed after crossing the cut. Although unique choice of the cut gives some advantages, the modification of the direction of "constant action" lines after crossing the cut make more difficult the analysis of the evolution of the elementary cell when crossing the cut.

The construction of the defect by removing a solid wedge leads to quite natural generalizations of the elementary monodromy defect. Instead of removing the solid wedge associated with elementary monodromy defect we can try to remove some fractional part of this wedge. This leads to two serious modifications. First of all, the points on two boundaries of the cut are not completely identical now and such construction should lead to line defect rather than to point defect as in the case of "elementary monodromy". Next point: the number of removed states from the regular lattice consists, in such a case, of two contributions, linear and oscillatory, depending on the fraction. Such quasi-polynomial dependence of the number of state function is known to be typical for problems with resonances [58, 51]. Formal construction of an example of $1:2$ defect associated with removing exactly a half of the solid wedge eliminated in the case of elementary monodromy is shown in figure 8. The specific feature of such defect is the fact, that the result of crossing such a defect by an elementary cell depends on the place where the cell crosses the cut. We can remove this ambiguity if we use instead of an elementary cell a double cell. From the point of view of standard Hamiltonian monodromy interpretation such construction suppose that instead of initial lattice (first homology group) we should use only sublattice (subgroup of index two in the case of $1:2$ fractional defect). Working only with subgroup, we have standard integer monodromy. At the same time, working with complete lattice we have new phenomenon, named fractional monodromy. The mathematical formulation of the fractional monodromy notion was done in [54, 55]. The completely new feature which appears together with introduction of fractional monodromy is the possibility to analyze the monodromy for contours

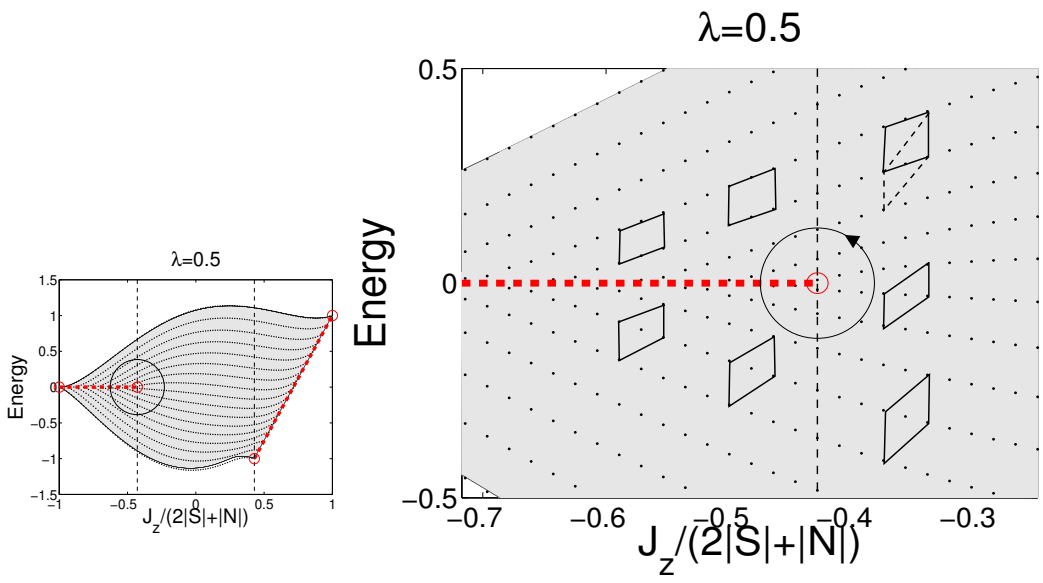

Figure 9: Coupling of angular momenta leading to fractional monodromy. Effective Hamiltonian is given by Eq. (2).

which cross singularities (codimension 1 strata formed by singular fibers). A typical singular fiber in the case of fractional monodromy is a curled torus, shown in figure 2, b. Different mathematical aspects of fractional monodromy notion are discussed in [53, 22, 29, 65].

The first example of concrete mathematical model leading to fractional Hamiltonian monodromy [54] used two non-linearly coupled oscillators with $1:(-2)$ resonance and with higher order terms which were introduced to ensure the compactness of the reduced phase space. Simple concrete model of angular momenta coupling, similar to model (1) was analyzed in [37]. The coupling between two angular momenta N_α and S_α simulate the $1:2$ resonance between vibrational modes:

$$H_\lambda = \frac{1-\lambda}{|\mathbf{S}|}S_z + \lambda\left(\frac{1}{|\mathbf{S}||\mathbf{N}|}S_zN_z + \frac{1}{2|\mathbf{S}||\mathbf{N}|^2}\left(N_-^2S_+ + N_+^2S_-\right)\right). \qquad (2)$$

The joint spectrum pattern corresponding to Hamiltonian (2) and to the intermediate value of control parameter $\lambda = 0.5$ is shown in figure 9. It clearly shows the presence of singular line with the end point (compare with figure 1, b). The fractional monodromy follows directly from the figure 9 by comparing the form of the initial and final double cells and expressing the result of the double cell evolution in terms of elementary cell transformation. More physical examples showing the presence of fractional monodromy in such simple quantum system as hydrogen atom in external electric and magnetic fields can be found in [24, 23].

4 3D-systems and monodromy

Extension of monodromy analysis from $2D$ to higher dimensional problems changes first of all the dimensionality of the subspace of critical values on the bifurcation diagram (on the image of the energy-momentum map). The codimension of the generic singular fiber (pinched torus) responsible for the elementary monodromy is equal to 2. This means that for $3D$-systems we have typically the whole lines (or rays) of singular values. Very interesting example of three-degree-of-freedom system with Hamiltonian monodromy is given by a resonant swing-spring (or elastic pendulum) [46, 47, 38, 20]. This is a three degree of freedom system (figure 10) with doubly degenerate swinging and non-degenerate springing and with the ratio $1:1:2$ between harmonic frequencies. This problem is practically identical to the famous Fermi resonance problem in CO_2 molecule which assumes exact

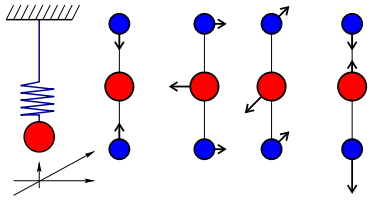

Figure 10: *Swing-spring* with 1:1:2 resonance (left) is a model of Fermi resonance in CO_2 molecule. Among four vibrational degrees of freedom of CO_2 molecule the symmetric stretching and doubly degenerate bending are in 2:1 resonance, whereas the antisymmetric stretching is out of resonance and can be effectively removed by normalization.

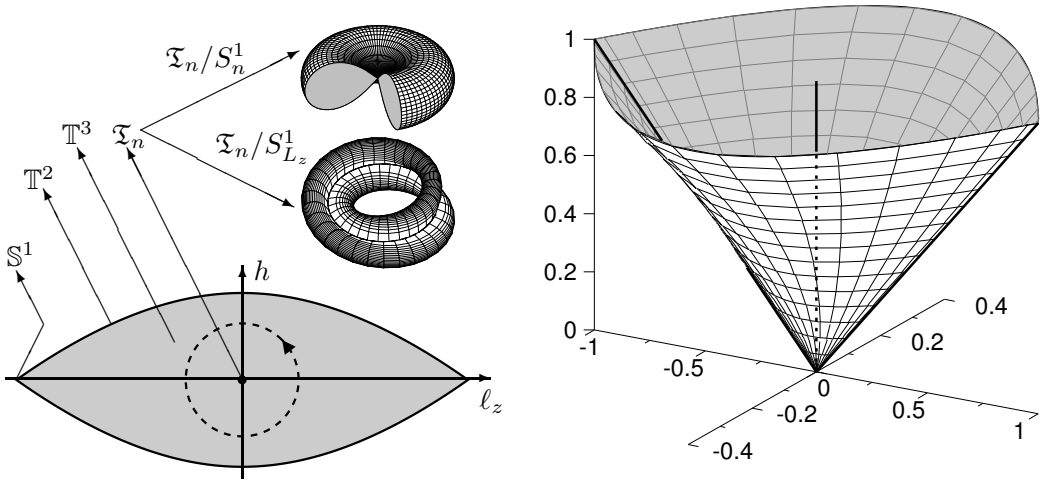

Figure 11: Image of the energy momentum map for the $1:1:2$ resonant oscillator system with axial symmetry (*and without detuning*). Full 3D-image, typical constant-n section and fibers.

$1:1:2$ resonance between doubly degenerate bending and symmetric stretching vibrations of CO_2 molecule.

The CO_2 molecules is naturally a quantum system. Thus the quantum version of swing-spring has an interesting physical meaning. The problem becomes integrable if we introduce the polyad quantum number (the total action for three harmonic oscillators in resonance in the classical model) as a good approximate quantum number. Axial symmetry of the problem together with energy conservation give three necessary integrals of motion. Three dimensional bifurcation diagram is presented in figure 11 [10, 30]. Line of singular values situated inside the "cone" of allowed values of the energy momentum map is responsible for nontrivial monodromy.

Corresponding quantum state lattice can be reconstructed from regular lattice by introducing simultaneously three elementary monodromy defects with different orientation (figure 12).

The transformation of the elementary cell going around the line of singular values is shown in details in figure 13. It is easy to verify that the cumulative effect of these three defects gives the monodromy matrix which belongs to the same class of conjugated elements of $SL(3,Z)$ as the "elementary monodromy" matrix. This nontrivial example shows utility of defect representation through solid wedge removing and the monodromy matrix calculation through evolution of an elementary cell. An interesting continuation of the present analysis of this quantum problem is the study of the plane switching phenomenon, observed in classical swing-spring [46, 47, 38], for quantum problem [61].

The above analysis of the CO_2 model (or swing-spring) was done under the assumption of the exact resonance condition $1:1:2$. At the same time a physically reasonable model should take into account the exact resonance condition between two degenerate by symmetry modes ($1:1$ resonance) and allow small detuning for $1:2$ ratio between stretching and bending vibrations. It is clear from

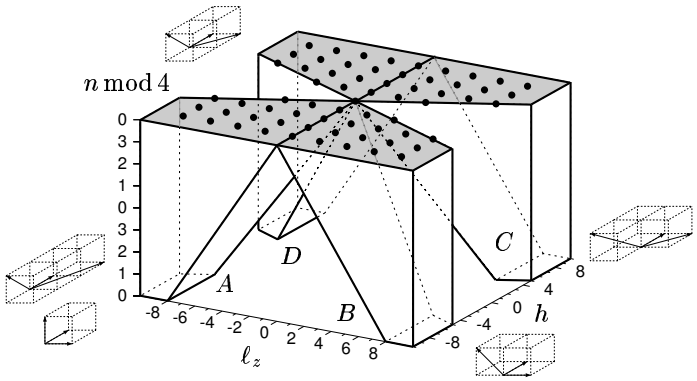

Figure 12: Quantum lattice with several elementary monodromy defects reproducing the joint spectrum for 1 : 1 : 2 resonant oscillators whose classical bifurcation diagram is shhown in figure 11.

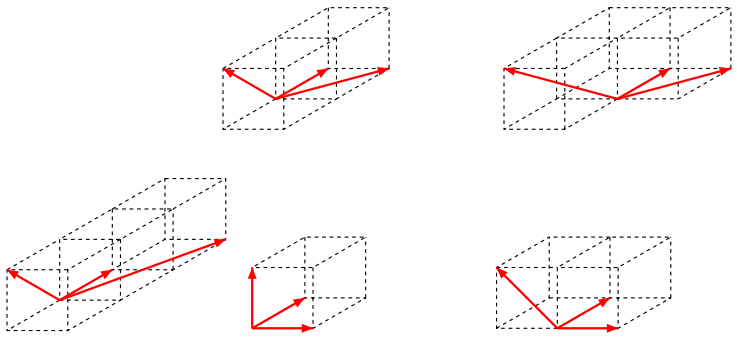

Figure 13: Details of the cell transformation during its transportation around line defect for quantum lattice with defects shown in figure 12.

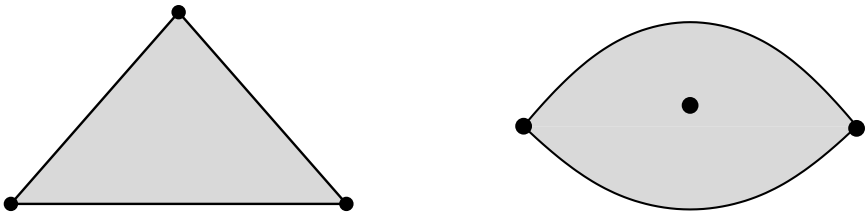

Figure 14: Hamiltonian systems with detuned 1:1:2 resonance. Manifestation of bidromy. Representation of the section of energy-momentum map in the case when detuning is more important (left) and when the resonance is more important (right).

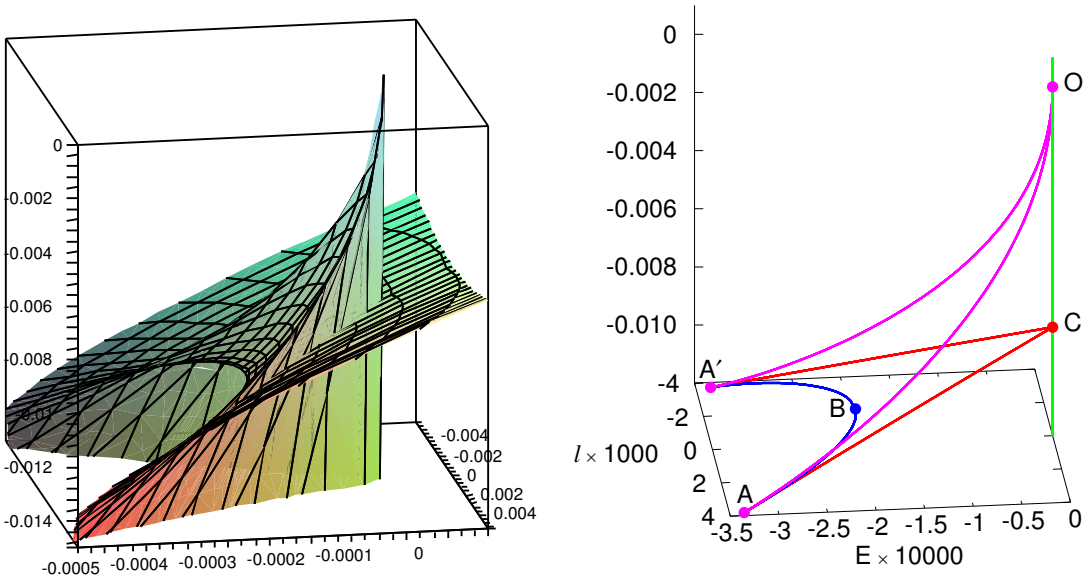

Figure 15: Essential part of the three-dimensional image of the energy-momentum map for $1:1:2$ resonant swing spring [60]. Two connected components of the inverse image of the energy-momentum map are present in the region $ABA'OC$ of the $3D$-bifurcation diagram. See text for further explanations.

simple qualitative arguments that in the case of relatively large detuning (as compare to splitting of $1:1:2$ polyads) the $n = const$ (n is a polyad quantum number) section of the image of the energy-momentum map should have a form of a triangle with three vertices corresponding to S^1 fibers (figure 14, left). At the same time, in the limit of negligible detuning the same $n = const$ section has the form shown in figure 14, right, possessing an isolated singular value. Taking the n as control parameter, it is reasonable to suppose that for small n the detuning should be large as compared to the splitting of the n shell, whereas for large n the splitting of n shell is more important because the detuning is largely independent on n and splitting grows rapidly with n. Thus, we conclude that with increasing n we should observe the Hamiltonian Hopf bifurcation. Careful analysis of the problem [60] shows that near the bifurcation point the image of the energy-momentum diagram becomes rather complicated (see figure 15).

The new region appears on the bifurcation diagram where two independent components of the inverse image of the energy momentum map are present. (This is the $ABA'OC$ region.) Moreover the global topological organization of components is quite special. Namely, starting on one connected component within the region $ABA'OC$, going out of this region through the $ABA'C$ face and returning back through any of two side faces AOC or $A'OC$, we can return back to the same point of the bifurcation diagram without crossing any singular tori but we finish the way on another connected component.

This peculiar situation was named the *bidromy* in [60]. This situation was found to be rather general, but little known. The illustration of the same type of global organization of connected components is shown on the example of integrable problem with two degrees of freedom in figure 16. Instead of standard bifurcation diagram this figure shows the so called unfolding surface which allows us to distinguish connected components of the inverse image of the energy-momentum map. Further details are given in [60, 25, 16].

5 Dynamical manifestation of monodromy

In his discussion [64] of the paper on the monodromy of swing-spring and CO_2 molecule [10] Ian Stewart formulates as the most tantalizing the possibility of detecting quantum monodromy experimentally.

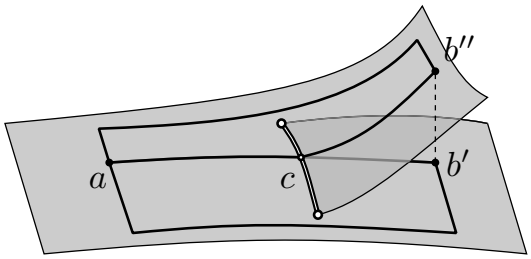

Figure 16: A single-sheet cell unfolding surface for the image of an energy momentum map with one self-overlapping lower cell: the inverse map can have one (point a) or two (points b' and b'') connected components. The path $b'ab''$ illustrates how it is possible to start on one connected component and going only through regular tori return back to the same point of bifurcation diagram but to another connected component.

The analogy between quantum Schrödinger cat and a classical falling cat turning himself upside down used by Stewart is not quite direct, but the idea to realize some time dependent physical process with the result showing directly the presence of monodromy and allowing even to measure the monodromy experimentally is obviously quite challenging.

All previous attempts with finding manifestation (or fingerprints) of monodromy in quantum systems was mainly related to the analysis of patterns formed by common eigenvalues of mutually commuting quantum operators. Such study reflects essentially the "static" character of quantum monodromy. In order to look for manifestation of monodromy during dynamic, time dependent processes we need first of all to formulate what kind of processes we need to realize and what kind of quantities we need to observe. The first step in this direction was done in [14, 15]. The authors use a very simple integrable problem with monodromy: a particle in a circular billiard with an axially symmetric potential of the form $U(r) = -ar^2$. Energy, E, and angular momentum, l, are two integrals of motion for this stationary problem. The image of the classical energy-momentum map has a singular value at $(E = 0, l = 0)$ point of bifurcation diagram. In order to see the "dynamical" manifestation of monodromy for this classical problem it is suggested to realize the time-dependent processes consisting of modification the energy, $E = E(t)$, and the angular momentum of the system, $l = l(t)$, in such a way that the parametric curve $(E(t), l(t))$ during the time interval $t_0 \leq t \leq t_f$ makes a closed path in the energy-momentum plane surrounding the singularity. We leave for a moment the question how to realize such a perturbation of the system and under what conditions we still can speak about energy and momentum as of integrals of motion even under presence of perturbation. We start with more intriguing question about the physical quantity which we need to observe in order to detect the presence of monodromy. The suggestion is to observe (instead of just one particle) the evolution of a number of particles moving in the same potential and perturbation and having different initial positions compatible with the same initial energy and angular momentum. From the formal point of view we can imagine a number of vehicles starting to move in a given billiard with a given potential and subjected to a given perturbation. We can choose the initial conditions in such a way that all vehicles are placed at different points on one radial line between inner and outer turning points defined by the given initial energy and having $l = 0$. We organize a perturbation in such a way that at each instant all vehicles have the same instantaneous energy and angular momentum values which follow the required $(E(t), l(t))$ dependence in the (E, l) plane. To force all vehicles to follow in a synchronize way through the same (E, l) points (i.e. to ensure that all particles belong to the same torus at any given time) is not an easy task. It is probably more easier to realize the same traffic with real vehicles by distributing in advance to all drivers the prescription where and when they should be located. But the result of this hypothetical evolution of a number of particles (or vehicles) is quite spectacular. It can be seen in figure 17 [15].

We need to compare the loop of initial conditions of a number of particles with the loop formed by all particles at the time when all particle finish their evolution in the (E, l) plane and return to the initial $(E, l = 0)$ point of the bifurcation diagram. Curiously, at the final moment all the particles

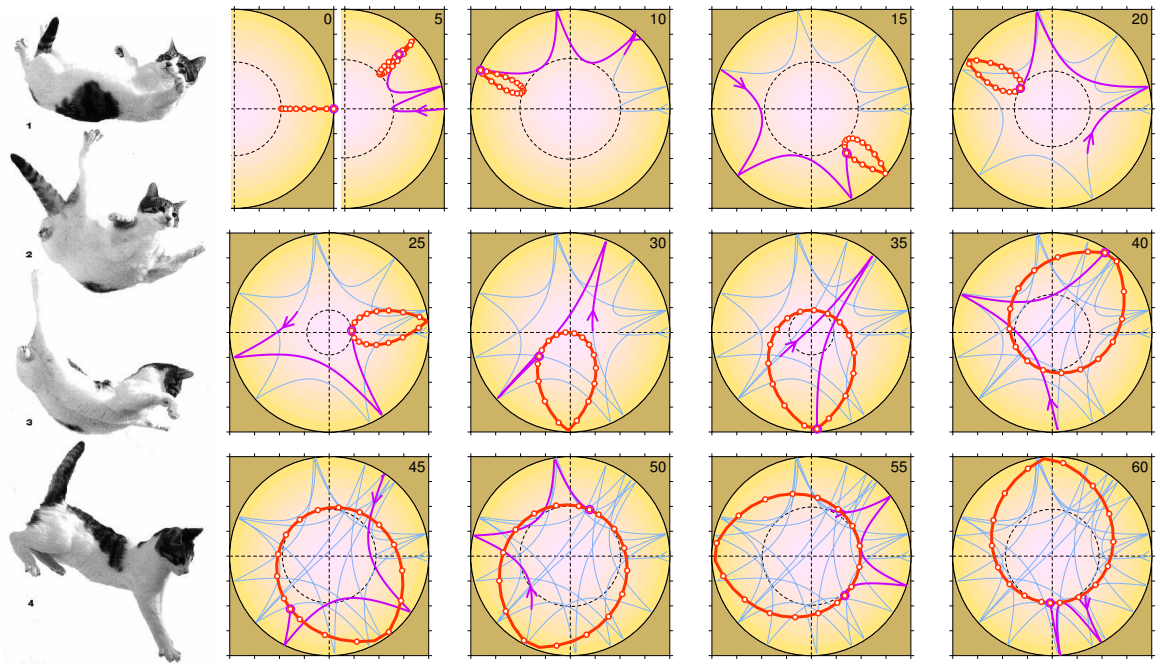

Figure 17: Dynamical evolution of the loop of initial condition of particles in circular billiard with $U \sim -r^2$ potential [15], as an alternative to falling cat analogy to Hamiltonian monodromy [64].

are distributed along a loop which encircles the central region of the billiard, forbidden for motion at final energy.

The topological nontrivial transformation of the loop of initial conditions for a series of particles into another topologically different loop of final positions is a direct consequence of the presence of monodromy for the problem considered.

How to realize such a processes and more precisely how to ensure the needed synchronized motion of different particles remains still an open problem. Nevertheless, the new idea, which seems to be important, is the possibility to look for the manifestation of monodromy by studying the behavior of an ensemble of particles. In fact, the big number of particles is not quite important for observation of monodromy. Even a pair of particles gives important information [15].

Note, that falling cat on the figure 17 is given just to refresh the analogy suggested by Stewart in [64].

6 Sign of monodromy

In order to discuss more general defects and more general monodromy matrices which can eventually appear in different problems we need first to be a little more precise about equivalence relation between different monodromy matrices and about the correspondence between monodromy matrices, topology of corresponding singular fibers, and defect construction. First, we repeat that monodromy matrices should be considered equivalent if they belong to the same class of conjugated elements of the $SL(2,Z)$ group (or $SL(n,Z)$ in the case of n-degrees of freedom systems). At the same time even in the case of $SL(2,Z)$ and $SL(3,Z)$ we can find a strange difference. For two degrees of freedom systems the two quite simple monodromy matrices

$$\begin{pmatrix} 1 & 0 \\ 1 & 1 \end{pmatrix}, \qquad \begin{pmatrix} 1 & 0 \\ -1 & 1 \end{pmatrix} \tag{3}$$

belong to different classes of conjugated elements within the $SL(2,Z)$ group. We name these matrices positive and negative elementary monodromy matrices. It is important to note that only one class

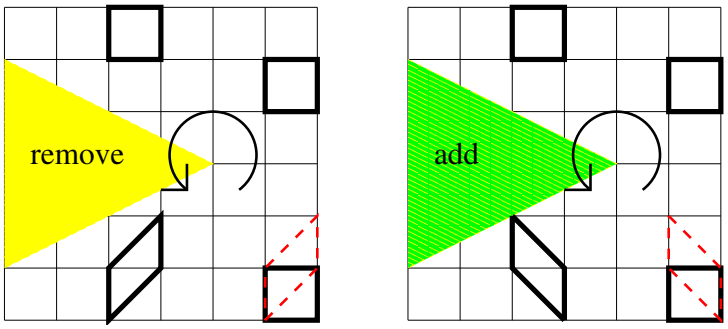

Figure 18: Comparison of elementary defects of different sign represented by *removing* or *adding* a wedge.

corresponds to an elementary toric singularity, the pinched torus. Its representation as a defect of a regular lattice corresponds to removing a wedge from the lattice and to identifying the wedge boundaries as it is shown in figure 7. From the point of view of "cut and glue" construction of defects, we could suggest the following procedure to create the defect with negative elementary monodromy matrix. Namely, after making a cut we can introduce the solid wedge into the lattice (instead of removing it) and identify the boundaries of the wedge with boundaries of the cut of the initial regular lattice (figure 18). Two patterns obtained by removing solid wedge and by adding the same solid wedge are easily distinguishable. It is sufficient to calculate the number of states as a function of one of integrals of motion. To do that, let us start by taking a part of initial regular lattice, where we want to remove or to add solid wedge. We always can chose this part in such a way that the number of states is a linear (even a constant) function of the value of integral of motion. After removing solid wedge, the number of states becomes always a convex function of the integral of the motion with the discontinuity of the slope indicating the position of the defect [19, 32, 70]. In contrast, if we add solid wedge the number of state function becomes a concave function, again with the discontinuity of the slope indicating the position of the defect.

At the same time in the case of three degree of freedom completely integrable systems the two monodromy matrices

$$\begin{pmatrix} 1 & 0 & 0 \\ 1 & 1 & 0 \\ 0 & 0 & 1 \end{pmatrix}, \qquad \begin{pmatrix} 1 & 0 & 0 \\ -1 & 1 & 0 \\ 0 & 0 & 1 \end{pmatrix} \tag{4}$$

belong to the same class of conjugated elements of $SL(3,Z)$ group. Nevertheless, from the point of view of defect construction by "cut and glue" procedure, changing two-dimensional lattice to three dimensional one is just a trivial extension to the third dimension. We can easily construct the line defect by removing a $3D$-solid wedge, or by adding a $3D$-solid wedge. The corresponding patterns are clearly distinguishable, while their monodromy matrices belong to same conjugacy class of $SL(3,Z)$ group and are, consequently, equivalent.

The conclusion of this comparison is: the monodromy matrix does not characterize completely the defect. One can imagine that as soon as we suggest for Hamiltonian systems the impossibility of existence of defects obtained by adding solid wedge, the elementary monodromy matrices with opposite sign cannot appear as a matrix characterizing the singularities of Hamiltonian systems. But the situation is slightly more complicated.

We need to allow for general Hamiltonian system the existence of multiple elementary singularities of the same sign and equivalently the simultaneous existence of many equivalent defects of regular lattice which all belong to the same class of conjugated elements of $SL(2,Z)$ group but have their simplest normal form in different bases. It is known [57, 13, 12], that an arbitrary matrix in $SL(2,Z)$ can be constructed as a cumulative monodromy matrix for a closed path surrounding multiple elementary focus-focus singularities, characterized each by elementary monodromy matrix of the same sign. In particular, by using 12 elementary monodromy singularities of the same sign and by choosing properly the basis for each of elementary monodromy matrix, we can find that monodromy matrix

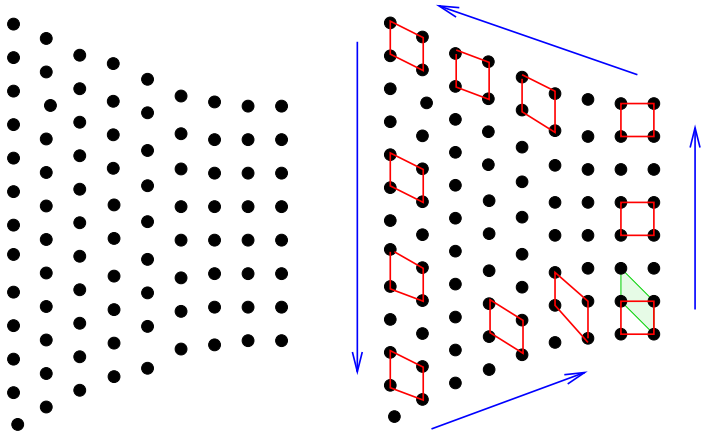

Figure 19: Example of the pattern impossible for Hamiltonian systems due to non-convexity of the image of the energy-momentum map.

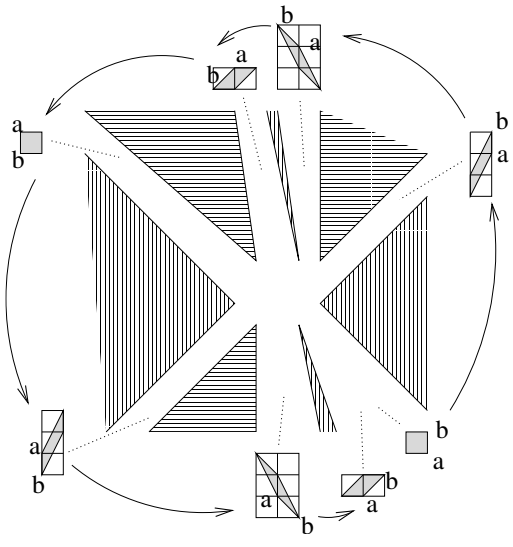

Figure 20: Cumulative effect of multiple (11) elementary defects [73].

for a contour surrounding all 12 singularities is the identity matrix. The identity monodromy matrix normally means that there is no monodromy, but the contour is obviously non-contractible and again we have an example when the monodromy matrix does not characterize the singularity.

Figure 20 gives an another example of a lattice with 11 elementary defects of the same type, corresponding each to removing an elementary solid wedge from the regular lattice [73]. These 11 elementary defects are arranged in such a way that the cumulative monodromy matrix has the sign opposite to the normal case. The same monodromy matrix could be produced by one elementary defect corresponding to adding a solid wedge to the lattice. It is clear that the monodromy matrix itself cannot characterize completely the singularity, or the defect of the lattice. In order to improve the situation we can add additional topological invariant characterizing singularities or defects.

Let us compare the evolution of the elementary cell along a closed path surrounding the singularity as shown in figures 19 and 20. During its circular path, the elementary cell on figure 20 realizes an extra 2π rotation around itself within the energy-momentum plane as compared with the evolution of the elementary cell in figure 19. Thus we can suggest the number of 2π rotations of an elementary cell as an additional invariant of the contour and of the singularity surrounded by this contour. Actually the author does not know examples of physically relevant dynamic systems which has singularities leading to non-zero number of 2π rotations of elementary cell. An interesting mathematical example was recently analyzed by Bolsinov, Dullin, Veselov [4], who have studied geodesic flow on *Sol*-manifolds. Their particular example of such manifold (which is a T^2 torus bundle over a circle with hyperbolic gluing map) leads to monodromy represented by the hyperbolic matrix $\begin{pmatrix} 1 & 1 \\ 1 & 2 \end{pmatrix}$. This matrix belong to the class of so called "cat maps", which according to [13] can be realized as a monodromy matrices of a closed path encircling 12 specially oriented elementary singularities. At the same time this monodromy matrix can be constructed as a cumulative effect of two elementary defects, one positive and one negative [73]. Two such constructions differ again by 2π rotation of the elementary cell during its way around the singularity. It should be noted that monodromy associated with singularity of a geodesic flow on *Sol*-manifold leads to 2π rotation, while the defect constructed from one positive and one negative elementary defects leads to zero number of 2π rotations. An interesting open question is: what kind of physical systems can manifest the presence of singularities characterized by a non-zero number of 2π-rotations of an elementary cell?

The simplest dynamical system which can allow the appearance of defects with nonzero number of 2π rotations of the elementary cell should allow the presence of at least 12 elementary monodromy defects. Looking at the list of almost toric symplectic four-manifolds [66, 45] the most interesting candidate is a K3 surface [31]. It appears as a total space of almost toric fibration over two-dimensional S^2 base space with 24 elementary singularities. This means that dynamic system with K3 phase space can be relevant as possible local model of nontrivial non-elementary singularities associated with new topological invariant, namely 2π rotation of the elementary cell along a closed path surrounding the singularity. In order to demonstrate the interest in such dynamic models we turn below in the next section to completely different examples of biological systems exhibiting so called spiral phyllotaxis phenomenon, which nevertheless seem to be quite related to discussed up to now monodromy and specific pattern formation.

Another interesting point related to the sign of monodromy matrix and to the sign of defect is the topological characterization of corresponding singular fiber. An elementary focus-focus singularity of a two degree of freedom Hamiltonian system is associated with a singular fiber which is a singly pinched torus. From the topological point of view a singly pinched torus is a sphere with one transversal self-intersection point with positive signature. As it is pointed by Matsumoto [48], there are two possibilities for such transversal self-intersection point. The signature of the self-intersection point can be positive or negative. In order to define whether the self-intersection is positive or negative, we need to start by defining a two-dimensional reference frame on a regular point of a fiber and to construct the 4D-reference frame at the self-intersection point by moving initial 2D-frame to critical point in two different non-equivalent ways. If the so defined 4D-frame corresponds to positive volume, the self-intersection is positive. If the volume of the 4D-space calculated with this 4D-frame is negative, the self-intersection is negative. What kind of dynamic system can lead generically to singular fiber which is a sphere with one transversal self intersection point of negative signature remains an open

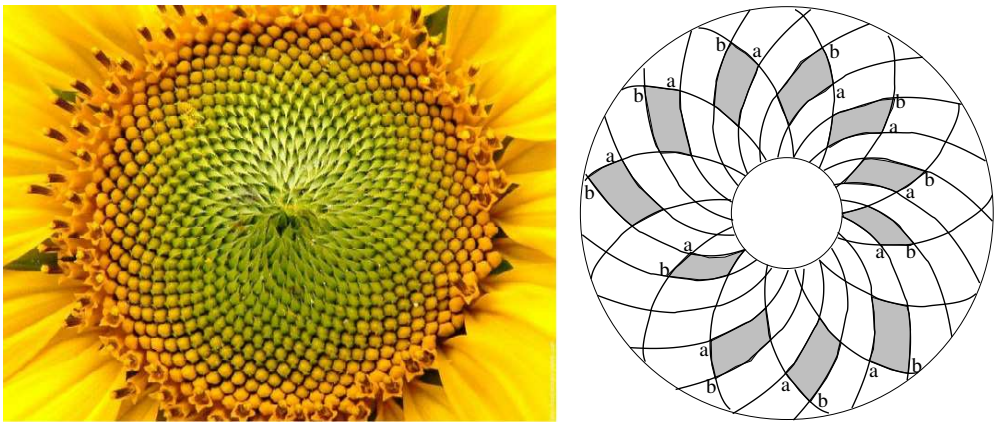

Figure 21: Sunflower with easily eye-guided 34 left and 55 right spires (parastichies) and similar lattice formed by 13 left and 21 right spires together with an elementary cell going around central singularity and exhibiting monodromy showing 2π rotation of the cell. To see better the rotation of the cell, two vertices of all cells are marked by letters a and b.

question [75].

7 Monodromy and sunflower

The notion of monodromy can be related to problems which are quite far from the classical Hamiltonian integrable systems, or model quantum molecules. The idea of such a generalization is based on the relation between defects of regular patterns and the monodromy. Namely, many defects of regular lattices which appear in solid state physics can be considered as a cumulative result of a number of elementary monodromy defects and can be treated as some complicated non-elementary defects from the point of view of monodromy defects. It is clear that the choice of "elementary bricks" is not unique. Even though the mathematical description of defects in solid state physics and in toric fibrations related to dynamical Hamiltonian systems, or in other models turns out to be similar, the relevance of these mathematical constructions should be confronted to physical reality.

We can try to generalize the mathematical description of defects in terms of elementary monodromy defects and to look from this point of view for typical singularities (defects) of almost regular patterns appearing in different domains. The general idea behind this is to find interpretation of defects in terms of natural "elementary ones" and to specify the generic most frequently appearing defects and to find a possible explanation of their appearance.

Regular patterns with defects can appear not only in solid state, with each point being associated with an atom or molecule, but in more complex systems like plants with regular patterns being associated with leaves or seeds, reflecting the morphogenesis or the plant development [67, 68]. The most striking example of such a regular pattern formation is the phyllotaxis, intriguing scientists working in different fields even quite far from biology. Let us just cite Leonardo da Vinci, Kepler, Bravais, Turing, Coxeter, .. [1].

The phenomenon of phyllotaxis describes the morphology of many botanical objects [39]. It exists in the arrangement of repeated units such as leaves around a stem in various plants, seeds of a pine-cones or of a sunflower, scales of a pineapple, etc. The most widely known is the spiral phyllotaxis [40, 62, 63] associated in a major part of cases with lattices formed by left hand and right hand spirals whose number are found to be consecutive numbers in the Fibonacci sequence $1, 1, 2, 3, 5, 8, ..., a_k, a_{k+1}, a_{k+2} = a_k + a_{k+1}, ...$ The interdisciplinary character of the phyllotaxis phenomenon is clearly seen on the example of pattern formation by drops of ferro-fluids in a magnetic field [17] or by flux lattices in superconductors [44].

Here we would like to bring attention of researchers to another aspect of phyllotaxis patterns which was not noted and discussed earlier up to our knowledge, namely its relation to monodromy of

lattices with defects and to singularities (Hamiltonian monodromy) of integrable dynamical systems or integrable fibrations in general.

Figure 21 shows real sun-flower with its easily seen spires formed by seeds. There are 55 right and 34 left spires. Locally seeds form an almost regular lattice which can be continued along a closed path surrounding the center of the flower. Similar lattice is reproduced on figure 21, right using another Fibonacci pair of right (21) and left (13) spires. Taking an elementary cell of this lattice and moving it around the center it is easy to see that the elementary cell returns to its original position after making a 2π rotation around itself. This means that the lattice formed by sunflower seeds has a singularity leading to trivial (identity) monodromy matrix and to non-trivial 2π rotation of the elementary cell with the direction of rotation corresponding to "normal" rotation. This means that the central singularity can be represented as a union of 12 "normal" elementary monodromy defects, arranged in such a way that they produce global identity monodromy matrix.

The choice of the sign of the monodromy defect observed for a wide range of botanic patterns seems to be rather fundamental property similar in the spirit to the left-right asymmetry and time irreversibility. A number of interesting questions naturally arise provoked by this supposition. Can the evolution of the plants be modeled by a dynamical system with the source being associated with a generic singularity characterized by an identity monodromy and positive 2π self-rotation? Does the sign of self-rotation reflect specific properties of the system?

References

[1] I. Adler, D. Barabe, and R.V. Jean. A History of the Study of Phyllotaxis. *Ann. Botany*, **80**, 231–244 (1997).

[2] V.I. Arnold. *Mathematical Methods of Classical Mechanics*. Springer, New York, 1989.

[3] L.M. Bates, Examples for obstructions to action-angle coordinates. Proc. Royal Soc. Edinburgh, **110**A, 27-30 (1988).

[4] A.V.Bolsinov, H.R.Dullin, A.P.Veselov, Spectra of Sol-Manifolds: Arithmetic and quantum monodromy. Commun.Math.Phys. **264**, 583-611 (2006).

[5] A. V. Bolsinov and A. T. Fomenko, *Integrable Hamiltonian systems. Geometry. Topology. Classifications*, Chapman & Hall/CRC, 2004,

[6] H.W. Broer, R.H. Cushman, F. Fassò, & F. Takens, Geometry of KAM-tori for nearly integrable Hamiltonian systems, *Ergod. Th. & Dynam. Sys.*, **27**, 725–741 (2007).

[7] M.S. Child, Quantum monodromy and molecular spectroscopy, Adv. Chem. Phys. **136**, 39–95 (2007).

[8] Cushman R.S. and Bates L., *Global aspects of classical integrable systems.* 1997, Basel, Germany: Birkhäuser.

[9] R. H. Cushman and J.J. Duistermaat, The quantum mechanical spherical pendulum. Bull. Am. Math. Soc. **19**, 475-479 (1988).

[10] R. Cushman, H. R. Dullin, A. Giacobbe, D. D. Holm, M. Joyeux, P. Lynch, D.A Sadovskii, B.Zhilinskii. CO_2 Molecule as a Quantum Realization of the $1:1:2$ Resonant Swing-Spring with Monodromy. Phys. Rev. Lett., **93**, 024302-1-4 (2004).

[11] R. H. Cushman and D. A. Sadovskii, Monodromy in the hydrogen atom in crossed fields, *Physica* D **142**, 166–196 (2000).

[12] R.H. Cushman and S.Vũ Ngọc. Sign of the monodromy for Liouville integrable systems. *Ann. H. Poincaré*, **3**, 883–894 (2002).

[13] R.H. Cushman and B. Zhilinskii Monodromy of two degrees of freedom Liouville integrable system with many focus-focus singular points. *J.Phys. A: Math. Gen*, **35**, L415–L419 (2002).

[14] J.B. Delos, G.Dhont, D.A. Sadovskii, B.I. Zhilinskii Dynamical manifestation of Hamiltonian monodromy, EPL, **83**, 24003-p1-6 (2008).

[15] J.B.Delos, G. Dhont, D.A. Sadovskii, and B. I. Zhilinski, Dynamical manifestations of Hamiltonian monodromy. Ann. Phys. (N.Y.) **324**, 1953-1982 (2009).

[16] G. Dhont, B.I. Zhilinskii Classical and quantum fold catastrophe in the presence of axial symmetry, Phys. Rev. A **78**, 052117-1-13 (2008).

[17] S. Douady and Y. Couder. Phyllotaxis as a physical self organized growth process. *Phys. Rev. Lett.*. **68**, 2098–2101 (1992).

[18] J.J. Duistermaat, On global action angle coordinates, *Comm. Pure Appl. Math.* **33**, 687-706 (1980).

[19] J.J. Duistermaat,G.L. Heckman, On the variation in the cohomology of the symplectic form of the reduced phase space, *Invent. Math.*, **69**, 259-268 (1982).

[20] H. Dullin, A. Giacobbe, and R. H. Cushman, Monodromy in the resonant swing–spring, Physica D **190**, 15–37 (2004).

[21] K. Efstathiou. *Metamorphoses of Hamiltonian systems with symmetry.* Lecture Notes in Mathematics, vol. 1864, Heidelberg: Springer-Verlag, 2004.

[22] Efstathiou K., Cushman R.H., and Sadovskii D.A., Fractional monodromy in the $1 : -2$ resonance. *Adv. Math.* **209**, 241–273 (2007).

[23] K. Efstathiou and D. Sadovskii, Normalization and global analysis of perturbations of the hydrogen atom. Rev. Mod. Phys. in press.

[24] K. Efstathiou, D.A. Sadovskii, and B.I. Zhilinskii. Classification of perturbations of the hydrogen atom by small static electric and magnetic fields. *Proc. Roy. Soc. A*, **463**, 1771–1790 (2007).

[25] K. Efstathiou and D. Sugny, Integrable Hamiltonian systems with swallowtails. J.Phys. A: Math. Gen. **43**, 085216 (2010).

[26] F. Faure and B. I. Zhilinskii, Topological Chern indices in molecular spectra, Phys. Rev. Lett. **85**, 960–963 (2000).

[27] Faure F. and Zhilinskii B. I., Topological properties of the Born-Oppenheimer approximation and implications for the exact spectrum. *Lett. Math. Phys.*, **55**, 219–238 (2001).

[28] F. Faure and B. I. Zhilinskii, Topologically coupled energy bands in molecules, Phys. Lett. A **302**, 242–252 (2002).

[29] A. Giacobbe. Fractional monodromy: parallel transport of homology cycles. *Diff. Geom. Appl.* **26**, 140-150 (2008).

[30] A. Giacobbe, R. H. Cushman, D. A. Sadovskiĭ, and B. I. Zhilinskiĭ, Monodromy of the quantum 1:1:2 resonant swing spring, *J. Math. Phys.*, **45**, 5076–5100 (2004).

[31] P.Griffiths and J. Harris, *Principles of algebraic geometry.* (New York: Wiley), 1978.

[32] L. Grondin, D. A. Sadovskiĭ, and B. I. Zhilinskiĭ, Monodromy in systems with coupled angular momenta and rearrangement of bands in quantum spectra, *Phys. Rev.* A **142**, 012105-1–15 (2002).

[33] M. Gross, Special Lagrangian Fibrations. I. Topology, in: *Integrable Systems and Algebraic Geometry*, Ed. by M.-H. Saito, Y. Shimuzu, and K. Ueno, World Scientific 1998, 156–193.

[34] M. Gross, Special Lagrangian Fibrations. II: Geometry, in: *Surveys in Differential Geometry*, Somerville, MA, International Press 1999, 341–403.

[35] M. Gross, Topological mirror symmetry, Invent. math. **144**, 75-137 (2001).

[36] Guillemin V., *Moment maps and combinatorial invariants of Hamiltonian T^n-spaces.* 1994, Basel, Birkhäuser.

[37] M.S. Hansen, F. Faure and B.I. Zhilinskii. Fractional monodromy in systems with coupled angular momenta. *J.Phys. A: Math. Theor.* **40**, 13075 (2007).

[38] D. D. Holm and P. Lynch, Stepwise precession of the resonant swinging spring, SIAM J. Applied Dyn. Syst. **1**, 44–64 (2002).

[39] R.V. Jean, Phyllotaxis: A Systematic Study in Plant Morphogenesis (Cambridge Univ. Press, Cambridge, UK, 1994).

[40] H. Jönsson, M. G. Heisler, B. E. Shapiro, E. M. Meyerowitz, and E. Mjolsness. An auxin-driven polarized transport model for phyllotaxis. *PNAS* **103**, 1633–1638 (2006).

[41] M. Kleman, *Points, Lines and Walls.* (Chichester: Wiley), 1983.

[42] E. Kroner, Continuum theory of defects, in *Physics of defects*. Les Houches, Ecole d'été de physique théorique, Elsevier, New York, 1981; pp. 215–315.

[43] L. M. Lerman and Ya. L. Umanskiĭ, *Four dimensional integrable Hamiltonian systems with simple singular points*, Transl. Math. Monographs **176**, American Math. Soc., Providence, R.I., 1998.

[44] L. S. Levitov. Phyllotaxis of Flux Lattices in Layered Superconductors. *Phys. Rev. Lett.* **66**, 224–227 (1991).

[45] N.C. Leung, M. Symington, Almost toric symplectic four-manifolds. arXiv:math.SG/0312165 (2003).

[46] P. Lynch, Resonant motions of the three-dimensional elastic pendulum, Intl. J. Nonlin. Mech. **37**, 345–367 (2002).

[47] P. Lynch and C. Houghton, Pulsation and precession of the resonant swinging spring, Physica D **190**, 38–62 (2004).

[48] Y. Matsumoto. Torus fibrations over the two sphere with the simplest singular fibers. *J. Math. Soc. Japan*, **37**, 605–636 (1985).

[49] V.S. Matveev. Integrable Hamiltonian Systems with two degrees of freedom. The topological structure of saturated neighborhoods of points of focus-focus and saddle-saddle type. *Sb. Math.*, **187**, 495–524 (1996).

[50] Mermin N.D., The topological theory of defects in ordered media, *Rev. Mod. Phys.*, **51**, 591–648 (1979).

[51] L. Michel and B. Zhilinskii, Symmetry, Invariants, and Topology. I. Basic Tools. Phys. Rep. **341**, 11-84 (2001).

[52] N.N. Nekhoroshev, Action-angle variables and their generalizations, *Trans. Moscow Math. Soc.*, **26**, 180–198 (1972).

[53] N.N. Nekhoroshev. Fractional monodromy in the case of arbitrary resonances. *Sbornic Mathematics*, **198**, 383–424 (2007).

[54] N. N. Nekhoroshev, D. A. Sadovskiĭ, and B. I. Zhilinskiĭ. Fractional monodromy of resonant classical and quantum oscillators. *C.R. Acad. Sci. Paris, Ser I* **335**, 985–988 (2002).

[55] N. N. Nekhoroshev, D. A. Sadovskií, and B. I. Zhilinskií, Fractional Hamiltonian monodromy, *Ann. Henri Poincaré* **7**, 1099–1211 (2006).

[56] Pavlov-Verevkin V. B., Sadovskii D.A. and Zhilinskii B.I., On the dynamical meaning of the diabolic points. *Europhys. Lett.*, **6**, 573–578 (1988).

[57] R. A. Rankin. *Modular forms and functions.* Cambridge Univ. Press, Cambridge, 1977.

[58] D. Sadovskii and B. Zhilinskii, Counting levels within vibrational polyads. Generating function approach, J. Chem. Phys. **103**, 10520-10536 (1995).

[59] D. A. Sadovskií and B. I. Zhilinskií, Monodromy, diabolic points, and angular momentum coupling, *Phys. Lett.*, A **256**, 235–244 (1999).

[60] D. Sadovskii and B. Zhilinskii, Hamiltonian systems with detuned 1 : 1 : 2 resonance. Manifestations of *bidromy*, *Ann. Phys. (N.Y.)*, **322**, 164–200 (2007).

[61] M. Sanrey, M. Joyeux, and D. A. Sadovski, Classical and quantum-mechanical plane switching in CO2, J. Chem. Phys. **124**, 074318 (2006).

[62] P.D. Shipman and A.C. Newell. Polygonal planforms and phyllotaxis on plants. *J. Theor. Biol.* **236**, 154-197 (2005).

[63] R.S. Smith, S. Guyomarc'h, T. Mandel, D. Reinhardt, C. Kuhlemeier, and P. Prusinkiewicz. A plausible model of phyllotaxis. *PNAS*, **103**, 1301-1306 (2006).

[64] I. Stewart, Quantizing the classical cat. Nature, **430**, 731-732 (2004).

[65] D. Sugny, P. Mardešić, M. Pelletier, A. Jebrane, and H.R. Jauslin. Fractional Hamiltonian monodromy from a Gauss-Manin monodromy. *J. Math. Phys.* **49**, 042701 (2008).

[66] M. Symington. Four dimensions from two in symplectic topology. in *Topology and Geometry of Manifolds*, Athens, GA, 2001, Proc. Symp. Pure Math., V. 71, AMS, Providence, RI, 153–208, 2003.

[67] R. Thom. Stabilité structurelle et morphogńèse. W.A.Benjamin, Inc. Reading Massachusetts, 1972

[68] A. Turing The Chemical Basis of Morphogenesis, Phil. Trans. Royal Soc. B **237**, 37-72 (1952).

[69] S. Vũ Ngọc. Quantum monodromy in integrable systems. *Comm. Math. Phys.*, **203**, 465–479 (1999).

[70] S. Vũ Ngọc. Moment polytopes for symplectic manifolds with monodromy. *Adv. Math.*, **208**, 909–934 (2007).

[71] van der Meer J.C., The Hamiltonian Hopf bifurcation. Lect. Notes Math, vol. 1160, Springer, New York, 1985.

[72] H. Waalkens, H.R. Dullin, and P.H. Richter, The problem of two fixed centers: bifurcations, actions, monodromy. Physica D, **196**, 265-310 (2004).

[73] B.I. Zhilinskii. Interpretation of quantum Hamiltonian monodromy in terms of lattice defects. *Acta Appl. Math.* **87**, 281-307 (2005).

[74] B. I. Zhilinskii, Hamiltonian monodromy as lattice defect, in: *Topology in Condensed matter*, Ed. M. Monastyrsky (Springer Series in Solid State Sciences, vol. **150**, 2006), p. 165–186.

[75] B. I. Zhilinski, Monodromy and complexity of quantum systems in: The Complexity of Dynamical Systems: A Multi-disciplinary Perspective. Eds. J. Dubbeldam, K. Green, and D. Lenstra, Wiley, in press.